RESEARCH ARTICLE

Diffusion Tensor Imaging in Male Premutation Carriers of the Fragile X Mental Retardation Gene

Ryu-ichiro Hashimoto, PhD,[1] Siddharth Srivastava, PhD,[2] Flora Tassone, PhD,[2,3] Randi J. Hagerman, MD,[2,4] and Susan M. Rivera, PhD[1,2,5]*

[1]Center for Mind and Brain, University of California, Davis, Davis, California, USA
[2]Medical Investigation of Neurodevelopmental Disorder (MIND), University of California, Davis, Sacramento, California, USA
[3]Department of Biochemistry and Molecular Medicine, University of California, Davis, Sacramento, California, USA
[4]Department of Pediatrics, University of California, Davis Medical Center, Sacramento, California, USA
[5]Department of Psychology, University of California, Davis, Davis, California, USA

ABSTRACT: Older male premutation carriers of the *FMR1* gene are associated with the risk of developing a late-onset neurodegenerative disorder, fragile X–associated tremor/ataxia syndrome. Although previous postmortem and in vivo magnetic resonance imaging studies have indicated white matter pathology, the regional selectivity of abnormalities, as well as their relationship with molecular variables of the *FMR1* gene, has not been investigated. In this study, we used diffusion tensor imaging to study male premutation carriers with and without fragile X–associated tremor/ataxia syndrome and healthy sex-matched controls. We performed a tract of interest analysis for fractional anisotropy and axial and radial diffusivities of major white matter tracts in the cerebellar–brain stem and limbic systems. Compared with healthy controls, patients with fragile X–associated tremor/ataxia syndrome showed significant reductions of fractional anisotropy in multiple white matter tracts, including the middle cerebellar peduncle, superior cerebellar peduncle, cerebral peduncle, and the fornix and stria terminalis. Significant reduction of fractional anisotropy in these tracts was confirmed by voxel-wise analysis using tract-based spatial statistics. Analysis of axial and radial diffusivities showed significant elevation of these measures in middle cerebellar peduncle, even among premutation carriers without fragile X–associated tremor/ataxia syndrome. Furthermore, regression analyses demonstrated a clear inverted U-shaped relationship between CGG-repeat size and axial and radial diffusivities in middle cerebellar peduncle. These results provide new evidence from diffusion tensor imaging for white matter abnormalities in the cerebellar–brain stem and limbic systems among individuals with the fragile X premutation and suggest the involvement of molecular mechanisms related to the *FMR1* gene in their white matter pathology.

Key Words: diffusion tensor imaging; cerebellum; *FMR1*; fragile X–associated tremor/ataxia syndrome

Fragile X–associated tremor/ataxia syndrome (FXTAS) is a late-onset neurodegenerative disorder that is caused by premutation expansions (55–200 CGG repeats) in the 5′ untranslated region of the fragile X mental retardation gene (*FMR1*).[1] Males have a higher risk of developing FXTAS than do females, with more than one third of male premutation carriers older than 50 years affected.[2] Although intention tremor and ataxia constitute the core clinical features of FXTAS, the main symptoms also include cognitive decline, autonomic dysfunction, neuropathy, and psychiatric features including anxiety, depression, and apathy.[3]

***Correspondence to:** Dr. Susan M. Rivera, Center for Mind and Brain, 202 Cousteau Place, Suite 250, Room 245, Davis, CA 95618, USA; srivera@ucdavis.edu

Relevant conflicts of interest/financial disclosures: The study was funded by NIH grants UL1DE019583, DA024854, and HD036071, NINDS grant RL1NS062412, and NIA grants RL1AG032119, RL1AG032115, and NCRR UL1 RR024146. Dr. Hagerman has received funding from Roche, Novartis, Seaside Therapeutics, Forest, Johnson and Johnson, and Neuropharm for treatment trials in fragile X or autism. There are no other potential conflicts of interest to report.
Full financial disclosures and author roles may be found in the online version of this article.

Received: 27 April 2010; **Revised:** 15 December 2010; **Accepted:** 24 December 2010
Published online 11 April 2011 in Wiley Online Library (wileyonlinelibrary.com). DOI: 10.1002/mds.23646

The pathogenetic mechanism of FXTAS is not yet fully understood. However, an RNA "toxic" gain-of-function model has been supported by several lines of evidence including the observation of abnormally elevated *FMR1* mRNA levels for premutation alleles.[4] Previous postmortem histological studies examined the pathological processes in the FXTAS brain and revealed eosinophilic intranuclear inclusions in neurons and astrocytes throughout the cerebrum and brain stem, with a particularly pronounced concentration in the hippocampus.[5] Prominent neuropathological features were also found in the cerebellum, including spongiform changes in deep cerebellar white matter.[5,6]

There have been only a few in vivo MRI morphometric studies that have examined brain pathology in patients with FXTAS. The T2 hyperintensity signal in the middle cerebellar peduncle and periventricular zones has been reported as a neuroradiological hallmark of FXTAS.[7] Our previous MRI study revealed volume reductions in the cerebrum, cerebellum, and brainstem in FXTAS.[8,9] Similarly, a previous voxel-based morphometry study on male premutation carriers revealed reduced voxel density in several brain regions, including the cerebellum and amygdalo-hippocampal complex.[10] Together with postmortem findings, the available evidence is suggestive of pronounced pathological changes in, but not limited to, the cerebellar–brain stem and limbic systems in premutation carriers.

In the present study, we used diffusion tensor imaging (DTI) technology to examine white matter abnormalities in male premutation carriers with and without FXTAS. DTI is a relatively new MRI tool for studying white matter microarchitecture.[11,12] Fractional anisotropy (FA) provides a useful measure of the degree of restriction of water diffusion in tract fibers. Recent studies indicated that axial diffusivity (magnitude of principal longitudinal diffusivity) and radial diffusivity (mean of diffusivity along the other two orthogonal directions) can also be informative because increases in the 2 measures may be selectively associated with different aspects of underlying white matter pathology, that is, axonal damage and demyelination.[13–15] Here, we employed an automated tract of interest (TOI) analysis for major white matter tracts in the cerebellar–brain and limbic systems using a White Matter Parcellation Map (WMPM).[16,17] To compare results across multiple methodologies, we also performed tract-based spatial statistics (TBSS), a recently developed voxel-based analysis of DTI data in which issues of misregistration can be greatly circumvented.[18] We further performed regression analyses using molecular measures of the *FMR1* gene, namely, CGG-repeat size and levels of mRNA elevation to examine the possible effects of these factors on white matter pathology.

Patients and Methods

Participants

We examined the brains of a total of 71 male participants for this study (age, 40–79 years): 20 healthy control (HC) participants, 35 participants with the premutation with FXTAS (PFX+), and 16 participants with the premutation without FXTAS (PFX−). The demographic information is summarized in Table 1. In this study, the premutation range was defined as those with a CGG-repeat size between 55 and 200. CGG-repeat size and *FMR1* mRNA were measured in each participant following the procedures described elsewhere.[19] There were 4 missing CGG-repeat size values (all in the HC group) and 7 missing mRNA values (6 HC and 1 PFX+). An F test and a subsequent post hoc test showed that the PFX+ group was significantly older than the PFX− group ($F = 4.65$, $P = .012$). For participants with CGG-repeat sizes within the premutation range, a trained physician (R.J.H.) scored the severity of FXTAS on a scale ranging from 0 to 6.[20] In this study, premutation carriers with FXTAS scores of 0 or 1 (borderline or questionable symptoms of tremor and/or ataxia) were automatically placed in the PFX− group, whereas those with FXTAS scores of 2 (clear tremor and/or ataxia) to 5 (severe tremor and/or ataxia and consistently using a wheelchair) were designated as PFX+. Subjects with the premutation were recruited through screening of fragile X pedigrees of probands with fragile X syndrome (48 families). Controls were recruited from the local community through the University of California, Davis Medical Center. All subjects gave their signed, written informed consent before participating in the study. The protocol was approved by the institutional review board at the University of California, Davis.

MRI Data Acquisition

All MRI data was acquired on a 1.5 T GE MR scanner (General Electric Medical Systems, Milwaukee, WI). Diffusion-weighted data were acquired using an echo planer imaging sequence with the following parameters: TR = 8000 ms, TE = 78 ms, field of view = 220 × 220 mm^2, in-plane resolution = 1.718 × 1.718 mm^2, 19 axial slices with 4 mm thickness, and 1-mm gap. The lowest slice was positioned at the bottom of the cerebellum to cover major white matter tracts in the cerebellum, brain stem, and limbic system. This resulted in including a portion of the corpus callosum within a scanning range in most cases. The diffusion weighting was applied along 6 directions using a b value of 1000 s/mm^2. In addition to 4 diffusion-weighted images per direction (4 × 6), 2 no-diffusion-weighted (b0) images were acquired at the beginning of the sequence, which resulted in 26 volumes per subject.

TABLE 1. Demographic data including molecular data for healthy control, premutation carriers affected with FXTAS, andunaffected premutation carriers

	Healthy control (HC) (n = 20)			Premutation with FXTAS (PFX+) (n = 35)			Premutation without FXTAS (PFX−) (n = 16)		
	Mean	SD	Range	Mean	SD	Range	Mean	SD	Range
Age[a]	60.2	9.2	40–79	65.5	7.57	47–78	58.2	10.4	42–78
FSIQ[b]	118.1	15.1	90–142	103.1	17.1	67–136	119.8	18.8	83–152
PIQ[b]	114.8	14.2	87–134	99.9	18.3	64–128	121.5	18.3	91–155
VIQ[c]	117.3	15.1	84–144	106.2	14.5	79–135	115.1	18.4	78–142
FXTAS score	NA			3.00	1.03	2–5	0.31	0.48	0–1
CGG repeat	29.31	3.75	18–35	94.8	19.1	59–133	94.1	32.5	55–166
FMR1 mRNA	1.27	0.33	0.63–1.85	3.28	0.79	1.75–5.25	3.16	0.94	1.86–4.7

[a]Significant main effect of group ($F = 4.65$, $P = .012$).
[b]Data were not available for 2 HCs and 2 PFX+. FSIQ, $F = 7.23$, $P = .002$; PIQ, $F = 9.78$, $P = .0002$.
[c]Data were not available for 2 HCs and 3 PFX+. VIQ, $F = 3.51$, $P = .036$.
SD, standard deviation; FSIQ, WAIS III Full-Scale IQ; PIQ, Performance IQ; VIQ, Verbal IQ.

DTI Data Analysis

We used the WMPM (http://cmrm.med.jhmi.edu/) for our automated TOI analysis. The analysis consisted of 3 parts: (1) calculate the FA and axial and radial diffusivity maps in the subject native space; (2) calculate the deformation field to transform the native space into the ICBM-152 space and apply the inverse deformation field to the WMPM; and (3) calculate the mean FA and axial and radial diffusivity values of each ROI using the WMPM transformed into the native space.

We used FMRIB's Diffusion Tool (FDT) in the FSL toolbox to generate the FA and axial and radial diffusivity images in the subject native space. First, the image series was corrected for eddy currents and head motion using affine registration to the first b0 volume. After correcting for the rotation parameters of head motion for each image, diffusion tensors were fitted independently to each voxel and served to calculate the FA and axial and radial diffusivity maps in the individual subject.

We used SPM5 to warp the WMPM into the subject native space. First, the mean b0 volume of the individual subject and its binary mask image was coregistered into the ICBM-152 space. We then normalized the coregistered b0 image into the ICBM-152 space and obtained the deformation field. We used the coregistered binary mask image when performing the normalization in order to prevent normalization outside the scanning range. We inversed the normalization process using the deformation utility included in the SPM5 package. The inversed field was applied to the WMPM to transform the ICBM standard space into the native subject space.

Of the 48 parcellated white matter tracts in the WMPM, 10 tracts of the cerebellar–brain stem and limbic systems were included in our TOIs: (1) middle cerebellar peduncle (MCP), (2) pontine crossing tract, (3) inferior cerebellar peduncle, (4) superior cerebellar peduncle, (5) corticospinal tract, (6) medial lemniscus (7) cerebral peduncle, (8) fornix (column and body of fornix), (9) fornix/stria terminalis, and (10) cingulum at the levels of the hippocampus. The 1–7 and 8–10 TOIs were classified to the cerebellar–brain stem system and the limbic system, respectively. For each TOI, we calculated mean FA and axial and radial diffusivity values from each individual using the transformed WMPM in the subject's native space. For this analysis, we used voxels with an FA value larger than 0.2 to exclude cortical gray matter and cerebral spinal fluid.[18,21,22] For comparison with the TOI analysis, we also performed TBSS analyses.[18] Statistically significant voxels were identified by threshold-free cluster enhancement,[23] with the threshold of family-wise error corrected $P < .05$ (see Supporting Information).

Results

TOI Analysis

Using the extracted FA and axial and radial diffusivity values in the TOIs, we performed separate 2-way analysis of covariance (ANCOVA) with group (HC, PFX+, PFX−) as an intersubject factor, DTI measure of TOIs (either FA, axial diffusivity, or radial diffusivity) as an intrasubject factor, and age as a covariate. There were highly significant main effects of group in all 3 measures (FA, $F = 9.75$, $P < .001$; axial diffusivity, $F = 14.57$, $P < .001$; radial diffusivity, $F = 16.67$, $P < .001$). For each DTI measure, we then performed follow-up 1-way ANCOVAs with age as a covariate to examine group differences in each individual TOI. The Benjamini–Hochberg method was implemented to adjust for the multiple statistical tests, with the false discovery rate set at 5%.[24] Results are summarized in Table 2. For TOIs in which a significant group effect was found, we performed post hoc analyses (Holm–Sidak test) to compare between 2 groups. Compared with HC, PFX+ showed significant alternations in all

TABLE 2. Group comparisons of fractional anisotropy (FA), axial diffusivity, and radial diffusivity in tracts of interest

	FA		Axial diffusivity		Radial diffusivity	
	F	*P*	*F*	*P*	*F*	*P*
Cerebellar and brain stem tracts						
MCP	7.53	.003[a]	23.29	<.001[x,y,z]	20.49	<.001[x,y,z]
R. Superior cerebellar peduncle	6.01	.010[a]	2.17	.16	4.87	.019[x]
L. Superior cerebellar peduncle	5.63	.011[a]	4.40	.030[x]	7.12	.004[x,y]
R. Inferior cerebellar peduncle	0.76	.532	4.06	.037[y]	3.97	.034[x]
L. Inferior cerebellar peduncle	1.35	.378	3.44	.059	5.22	.015[x]
Pontine crossing tract	2.54	.134	0.51	.600	0.38	.160
R. Cerebral peduncle	10.20	<.001[a]	13.22	<.001[x]	20.01	<.001[x,y,z]
L. Cerebral peduncle	4.72	.023[a]	17.26	<.001[x,y]	14.7	<.001[x,y]
R. Corticospinal tract	2.72	.124	4.73	.025[x]	6.95	.017[x]
L. Corticospinal tract	1.02	.447	5.20	.019[x]	4.19	.029[x]
R. Medial lemniscus	1.55	.317	0.54	.624	1.16	.338
L. Medial lemniscus	1.02	.48	0.58	.640	1.84	.188
Limbic tracts						
Fornix	9.70	<.001[a,c]	7.26	.009[x]	8.35	.002[x]
R. Cingulum at the levels of hippocampus	0.41	.664	0.90	.502	1.12	.333
L. Cingulum at the levels of hippocampus	0.72	.523	2.29	.156	3.57	.044
R. Fornix/stria terminalis	11.00	<.001[a]	5.50	.017[x]	8.52	.003[x]
L. Fornix/stria terminalis	14.42	<.001[a,c]	8.64	.002[x]	12.27	<.001[x,z]

[a–c, x–z]Significant group difference identified by a post hoc test (Holm–Sidak test, $P < .05$); [a]HC > PFX+; [b]HC > PFX−; [c]PFX− > PFX+; [x]HC < PFX+; [y]HC < PFX−; [z]PFX− < PFX+;*F*, *F* value; *P*, *P* value; HC, healthy control; PFX+, premutation carriers with FXTAS; PFX−, premutation carriers without FXTAS; MCP, middle cerebellar peduncle; L, left; R, right.

3 measures in the MCP, left superior cerebellar peduncle, bilateral cerebral peduncle, fornix, and bilateral fornix/stria terminalis (Table 2). Although FA did not show significant difference between HC and PFX− in any TOI, significant increases in axial and radial diffusivities for PFX− were identified in MCP and left cerebral peduncle (see Fig. 1 for individual plots of the 3 DTI measures in 2 representative TOIs: the MCP and right cingulum at the levels of hippocampus).

TBSS Analysis

In the TBSS analysis, contrasting HC with PFX+ revealed significant FA reductions for patients in multiple tracts in the cerebellar–brain stem and limbic systems as well as other white matter tracts (Fig. 2A). Table 3 summarizes significant voxels in the cerebellar–brain stem and limbic systems. All the TOIs that showed significant FA reduction in the TOI analysis were replicated in this analysis. There was no voxel that showed larger FA in PFX+ than in HC. In contrasting PFX− with PFX+, voxels with significant FA reduction were found in the fornix and fornix/stria terminalis in the limbic system, which replicated the TOI analysis, and in other white matter tracts such as the splenium of the corpus callosum and posterior thalamic radiation (Fig. 2B and Table 3). No significant voxel showed PFX+ > PFX−. In contrasting HC with PFX−, no significant voxels were identified in either direction, consistent with TOI analysis. There was no significant voxel identified by simple regression analysis using either CGG-repeat size or *FMR1* mRNA level. In regression analysis using the FXTAS score, clusters with a significant negative effect were found in multiple tracts including the fornix and the MCP (Fig. 2C and Table 3). Progressive pathological alternations in these tracts were also identified by significant positive correlation between the FXTAS score and either axial or radial diffusivity (see Supporting Information Table S1).

Correlation Analysis Using Molecular Variables for DTI Measures in MCP

Among DTI measures in the TOIs, significant reductions in axial and radial diffusivities in the MCPs of premutation carriers are particularly noticeable (Table 2), indicating significant pathological processes in this tract. To investigate possible underlying molecular mechanisms, we performed regression analyses using CGG-repeat size and *FMR1* mRNA expression for axial and radial diffusivities in the MCP, combining PFX+ and PFX−. We found clear quadratic relationships of CGG-repeat size with both axial and radial diffusivities (Fig. 3). A trend-level positive correlation was found between *FMR1* mRNA expression and axial diffusivity ($r = 0.26$; $P = .068$), whereas there was no clear correlation with radial diffusivity ($r = 0.176$; $P = .223$).

Discussion

We found clear evidence of abnormalities in white matter integrity in the male premutation carriers with

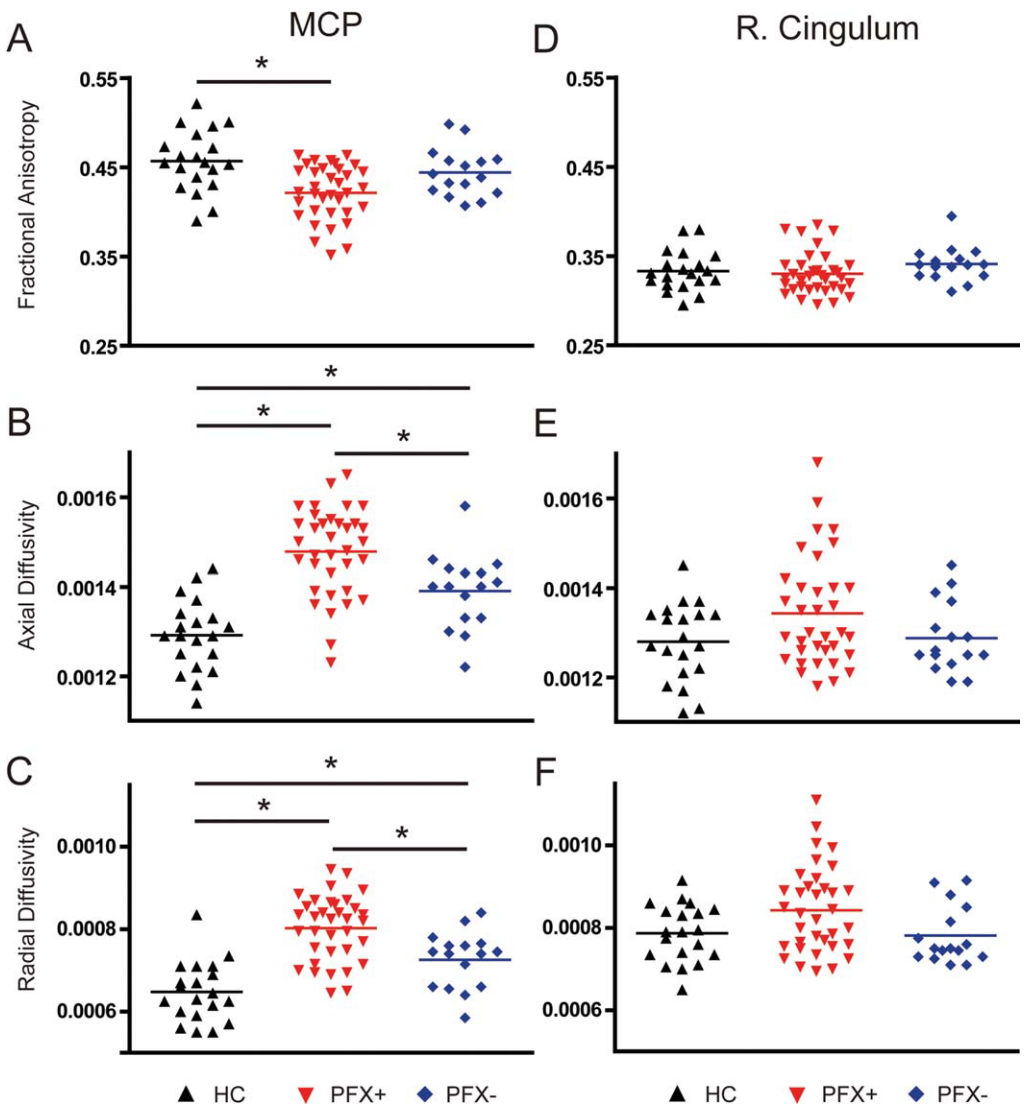

FIG. 1. Group comparisons of fractional anisotropy (FA), axial diffusivity, and radial diffusivity. **A–C:** Middle cerebellar peduncle (MCP). **D–F:** Right cingulum at the levels of the hippocampus. Asterisks indicate significant group difference ($P < .05$) indicated by a post hoc test (Holm–Sidak test).

FXTAS. These individuals demonstrated marked reductions of FA in multiple white matter tracts: the MCP, superior cerebellar peduncle, and cerebral peduncle in the cerebellar–brain stem system and the fornix and fornix/stria terminalis in the limbic system. FA reductions in these tracts were replicated in TBSS analyses. Axial and radial diffusivity values in the MCP and cerebral peduncle in both hemispheres were found to be increased in the unaffected premutation carriers, indicating incipient white matter pathology before the onset of major symptoms. Regression analyses using molecular measures of the *FMR1* gene demonstrated clear inverted U-shaped relationships between CGG-repeat size and axial and radial diffusivities in the MCP. To our knowledge, the present study represents the first evidence using DTI for assessing abnormalities in specific white matter tracts of *FMR1* premutation carriers with and without FXTAS, together with the effects of the *FMR1* molecular variables on alternations of white matter microstructure in these individuals.

Our analysis of FA values of the cerebellar peduncles indicated significant pathological processes in the MCP and superior cerebellar peduncles, which corresponded to major afferent and efferent fibers of the cerebellum, respectively. It is possible that reduced FA values in the superior cerebellar peduncle reflect deficient output from the cerebellum, as evidenced by neuropathological features of Purkinje cells in patients with FXTAS.[6] It is also noteworthy that in the unaffected premutation carriers, significant alternations of the MCP were identified only by axial and radial diffusivities but not by FA (Table 2). A similar observation was described by a recent DTI study that reported better utility of axial and radial diffusivities than FA as markers of neurodegeneration in amyotrophic lateral sclerosis.[25] However, it remains unknown whether axial and radial diffusivities have better

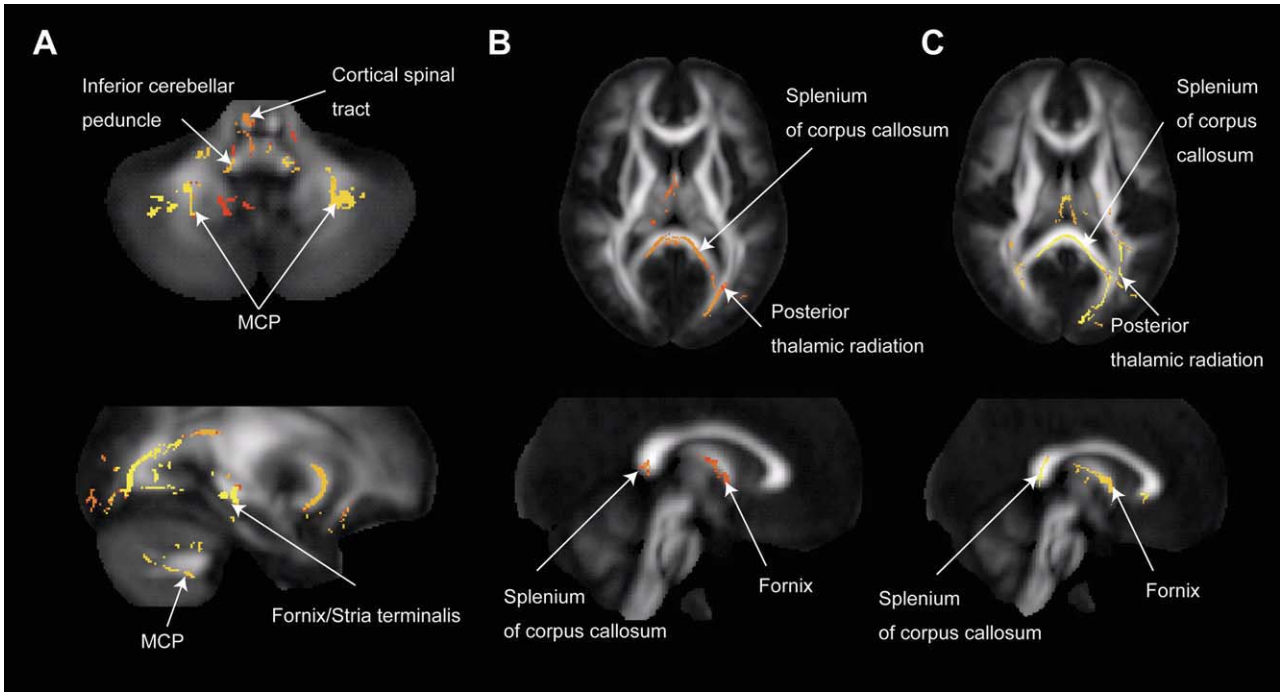

FIG. 2. Significant reduction of fractional anisotropy (FA) related to FXTAS identified by TBSS analysis. **A:** Significant FA reduction in patients with FXTAS identified by HC versus PFX+ in the MNI space. **B:** Significant FA reduction in patients with FXTAS identified by PFX− versus PFX+. **C:** Significant FA reduction correlated with FXTAS score. MCP, middle cerebellar peduncle.

sensitivity for degenerative processes of *FMRI* premutation carriers in general or only for those occurring in specific white matter tracts.

In the brain stem, the cerebral peduncle showed significant FA reduction in the patients with FXTAS, although the bilateral corticospinal tract showed altered axial and radial diffusivities. In the WMPM, the boundary between the cerebral peduncle and corticospinal tract was set around the boundary between the mesencephalon and the pons. Our observation is partly consistent with previous clinical MRI studies reporting the volume loss of the

TABLE 3. Significant voxels in the cerebellar, brain stem, and limbic tracts identified by TBSS analysis

	HC > PFX+					PFX− > PFX+					Negative correlation with FXTAS score				
	x	y	z	*P*	Volume (mm^3)	x	y	z	*P*	Volume (mm^3)	x	y	z	*P*	Volume (mm^3)
Cerebellar and brain stem tracts															
MCP	33	−50	−40	.002	1085			NS			32	−52	−43	.033	71
R. Superior cerebellar peduncle	10	−51	−31	.011	171			NS					NS		
L. Superior cerebellar peduncle	−6	−53	−31	.010	190			NS					NS		
R. Inferior cerebellar peduncle	11	−45	−34	.011	122			NS					NS		
L. Inferior cerebellar peduncle	−6	−54	−21	.010	144			NS					NS		
Pontine crossing tract	7	−29	−30	.019	31			NS					NS		
R. Cerebral peduncle	9	−7	−7	.005	369			NS			15	−10	−6	.022	123
L. Cerebral peduncle	−19	−21	−7	.0002	253			NS			−18	−21	−5	.007	93
R. Corticospinal tract	4	−20	−32	.014	215			NS					NS		
L. Corticospinal tract	−5	−18	−24	.012	51			NS					NS		
R. Medial lemniscus	7	−39	−28	.011	110			NS					NS		
L. Medial lemniscus	−6	−39	−28	.011	81			NS					NS		
Limbic tracts															
Fornix	2	−13	15	.0002	78	1	−4	9	.036	67	1	−5	9	.01	87
R. Cingulum (hippocampal levels)	25	−29	−12	.0004	85	13	−47	7	.029	10	14	−45	7	.0004	208
L. Cingulum (hippocampal levels)	−15	−46	1	.0002	253	−14	−43	2	.026	17	−11	−45	2	.0004	221
R. Fornix/Stria terminalis	31	−26	−10	.0002	119			NS			31	−22	−8	.016	208
L. Fornix/Stria terminalis	−23	−35	2	.0002	159	−25	−35	2	.028	9	−28	−25	−10	.004	143

HC, healthy control; PFX+, premutation carriers with FXTAS; PFX−, premutation carriers without FXTAS; MCP, middle cerebellar peduncle; L, left; R, right; NS, no significant voxel was identified.

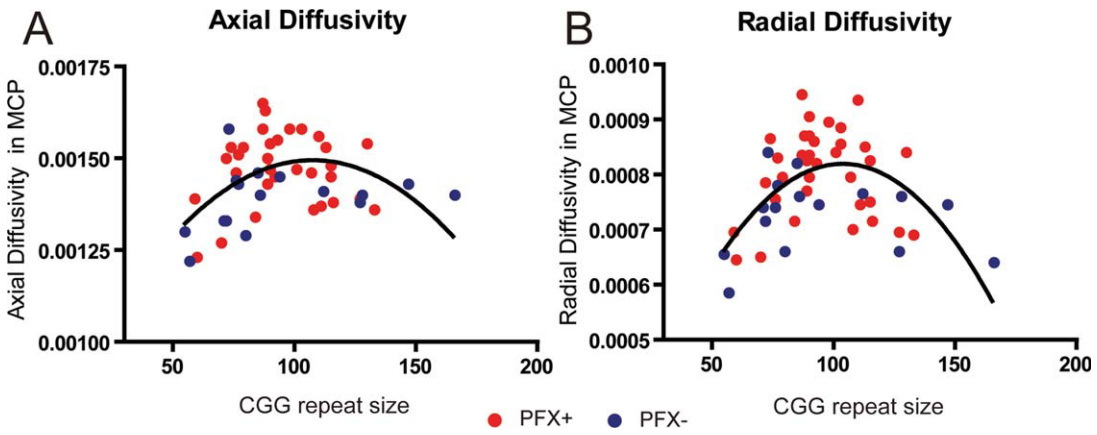

FIG. 3. Inverted U-shaped relationships between CGG repeat size and axial and radial diffusivity in the middle cerebellar peduncle (MCP) among premutation carriers. The quadratic relationship was highly significant for axial diffusivity (r^2 = 0.238, P = .001) and radial diffusivity (r^2 = 0.363, P < .001).

mesencephalon and pons in patients with FXTAS as well as reduced volume reduction in the total brain stem in both affected and unaffected premutation carriers.[7,8] FA values of the MCP and cerebral peduncle showed significant negative correlation with the severity of FXTAS (Table 3), indicating progressive pathological changes in the cerebellar and brain stem tracts.

In the limbic system, we observed significant alternations of FA and axial and radial diffusivities in the fornix and the bilateral fornix/stria terminalis in patients with FXTAS (Table 2). It is possible that abnormalities in these tracts may underlie psychiatric and psychological problems, such as depression and anxiety, and autonomic dysfunction in patients with FXTAS.[26–29] In TBSS analyses, the contrast of PFX− versus PFX+ and regression analysis using the FXTAS score showed significant clusters in these limbic TOIs (Fig. 2B,C and Table 3). These alternations may underlie progressive deterioration of cognitive and psychological functions over the progress of FXTAS.

Our analysis using *FMR1* molecular variables demonstrated a quadratic relationship between CGG-repeat size and axial and radial diffusivities in the MCP. Our findings imply that a different pathogenic mechanism in white matter may be at play for premutation carriers in the high-repeat range. It is possible that a deficit in FMR1 protein expression starts to play a "protective role" in high-repeat carriers, for whom translational efficiency has been shown to decrease in the upper premutation range.[30,31] For individuals in this range, then, the neurotoxic effect of elevated mRNA may be somewhat ameliorated. A less severe pathological process in the high-repeat range was also indicated by analysis of FA (see Supporting Information Fig. S1). Previous studies indicated that axial and radial diffusivities are selectively associated with axonal damage and demyelination, respectively,[13–15] and past postmortem studies identified various forms of axonal and myelination abnormalities in the cerebellums of those with FXTAS. It would be interesting to examine in future postmortem and animal model studies the possible nonlinear relationship between CGG-repeat size and pathological features of axon and myelin by including FMRP measures.

Recent studies have made remarkable progress in the development of protocols for the tractography of major fibers in the cerebellar and limbic systems.[32–36] Such tractographic approaches can be particularly powerful for the FXTAS brain, as evidenced by successful identification of individual cerebellar peduncles in cerebellar neurodegenerative diseases.[37] However, tractographic approaches were not optimal for our DTI parameter settings regarding the number of diffusion encoding directions as well as spatial resolution. As a complementary approach, we adopted TBSS analysis that replicated significant FA reductions in FXTAS obtained by our automated TOI analysis. On the other hand, TBSS detected significant alternations in tracts where TOI analysis did not find significant difference, including the inferior cerebellar peduncle and cingulum at the levels of the hippocampus (Tables 2 and 3). We therefore suggest that our findings regarding those white matter tracts need to be reassessed by future studies adopting tractographic and manual drawing methods. We also note that according to our previous study, volumetric measures of cerebral and cerebellar volumes and white matter volumes were comparable in control and unaffected premutation males.[8] Therefore, it is unlikely that misregistration caused by general brain atrophy explains our findings, particularly about the MCP, where significant alternations of axial and radial diffusivities were found, even in the unaffected premutation individuals.

To conclude, this study has presented evidence from DTI for reduced white matter integrity in the cerebella–brain stem and limbic systems of male carriers of *FMR1* premutation alleles. Our findings that white

matter abnormalities in the MCP are not only observable in patients with FXTAS but are already present even in unaffected premutation carriers is very significant and holds promise for the possibility of identifying patients for early targeted treatments for FXTAS. Future studies targeting the other critical white matter tracts will further advance our understanding of the neural bases of the various behavioral abnormalities of this genotype. ■

Acknowledgments: We thank Patrick Adams, who assisted with the MRI data collection, and most especially the individuals who participated in our brain imaging studies.

References

1. Hagerman RJ, Leehey M, Heinrichs W, et al. Intention tremor, parkinsonism, and generalized brain atrophy in male carriers of fragile X. Neurology. 2001;57:127–130.
2. Jacquemont S, Hagerman RJ, Leehey MA, et al. Penetrance of the fragile X-associated tremor/ataxia syndrome in a premutation carrier population. JAMA. 2004;291:460–469.
3. Amiri K, Hagerman RJ, Hagerman PJ. Fragile X-associated tremor/ataxia syndrome: an aging face of the fragile X gene. Arch Neurol. 2008;65:19–25.
4. Hagerman PJ, Hagerman RJ. The fragile-X premutation: a maturing perspective. Am J Hum Genet. 2004;74:805–816.
5. Greco CM, Hagerman RJ, Tassone F, et al. Neuronal intranuclear inclusions in a new cerebellar tremor/ataxia syndrome among fragile X carriers. Brain. 2002;125:1760–1771.
6. Greco CM, Berman RF, Martin RM, et al. Neuropathology of fragile X-associated tremor/ataxia syndrome (FXTAS). Brain. 2006;129:243–255.
7. Brunberg JA, Jacquemont S, Hagerman RJ, et al. Fragile X premutation carriers: characteristic MR imaging findings of adult male patients with progressive cerebellar and cognitive dysfunction. AJNR Am J Neuroradiol. 2002;23:1757–1766.
8. Cohen S, Masyn K, Adams J, et al. Molecular and imaging correlates of the fragile X-associated tremor/ataxia syndrome. Neurology. 2006;67:1426–1431.
9. Adams JS, Adams PE, Nguyen D, et al. Volumetric brain changes in females with fragile X-associated tremor/ataxia syndrome (FXTAS). Neurology. 2007;69:851–859.
10. Moore CJ, Daly EM, Tassone F, et al. The effect of pre-mutation of X chromosome CGG trinucleotide repeats on brain anatomy. Brain. 2004;127:2672–2681.
11. Le Bihan D. Looking into the functional architecture of the brain with diffusion MRI. Nat Rev Neurosci. 2003;4:469–480.
12. Mori S, Zhang J. Principles of diffusion tensor imaging and its applications to basic neuroscience research. Neuron. 2006;51:527–539.
13. Song SK, Sun SW, Ju WK, Lin SJ, Cross AH, Neufeld AH. Diffusion tensor imaging detects and differentiates axon and myelin degeneration in mouse optic nerve after retinal ischemia. Neuroimage. 2003;20:1714–1722.
14. Song SK, Yoshino J, Le TQ, et al. Demyelination increases radial diffusivity in corpus callosum of mouse brain. Neuroimage. 2005; 26:132–140.
15. Budde MD, Xie M, Cross AH, Song SK. Axial diffusivity is the primary correlate of axonal injury in the experimental autoimmune encephalomyelitis spinal cord: a quantitative pixelwise analysis. J Neurosci. 2009;29:2805–2813.
16. Hua K, Zhang J, Wakana S, et al. Tract probability maps in stereotaxic spaces: analyses of white matter anatomy and tract-specific quantification. Neuroimage. 2008;39:336–347.
17. Wakana S, Caprihan A, Panzenboeck MM, et al. Reproducibility of quantitative tractography methods applied to cerebral white matter. Neuroimage. 2007;36:630–644.
18. Smith SM, Jenkinson M, Johansen-Berg H, et al. Tract-based spatial statistics: voxelwise analysis of multi-subject diffusion data. Neuroimage. 2006;31:1487–1505.
19. Tassone F, Hagerman RJ, Garcia-Arocena D, Khandjian EW, Greco CM, Hagerman PJ. Intranuclear inclusions in neural cells with premutation alleles in fragile X associated tremor/ataxia syndrome. J Med Genet. 2004;41:e43.
20. Jacquemont S, Hagerman RJ, Leehey M, et al. Fragile X premutation tremor/ataxia syndrome: molecular, clinical, and neuroimaging correlates. Am J Hum Genet. 2003;72:869–878.
21. Snook L, Plewes C, Beaulieu C. Voxel based versus region of interest analysis in diffusion tensor imaging of neurodevelopment. Neuroimage. 2007;34:243–252.
22. Bonekamp D, Nagae LM, Degaonkar M, et al. Diffusion tensor imaging in children and adolescents: reproducibility, hemispheric, and age-related differences. Neuroimage. 2007;34:733–742.
23. Smith SM, Nichols TE. Threshold-free cluster enhancement: addressing problems of smoothing, threshold dependence and localisation in cluster inference. Neuroimage. 2009;44:83–98.
24. Benjamini Y, Hochberg Y. Controlling the false discovery rate: a practical and powerful approach to multiple testing. J R Stat Soc Series B Stat Methodol. 1995;57:289–300.
25. Metwalli NS, Benatar M, Nair G, et al. Utility of axial and radial diffusivity from diffusion tensor MRI as markers of neurodegeneration in amyotrophic lateral sclerosis. Brain Res. 2010;1348:156–164.
26. Hessl D, Tassone F, Loesch DZ, et al. Abnormal elevation of FMR1 mRNA is associated with psychological symptoms in individuals with the fragile X premutation. Am J Med Genet B Neuropsychiatr Genet. 2005;139B:115–121.
27. Bourgeois JA, Coffey SM, Rivera SM, et al. A review of fragile X premutation disorders: expanding the psychiatric perspective. J Clin Psychiatry. 2009;70:852–862.
28. Berry-Kravis E, Goetz CG, Leehey MA, et al. Neuropathic features in fragile X premutation carriers. Am J Med Genet. 2007;143:19–26.
29. Roberts JE, Bailey DB,Jr., Mankowski J, et al. Mood and anxiety disorders in females with the FMR1 premutation. Am J Med Genet B Neuropsychiatr Genet. 2009;150B:130–139.
30. Tassone F, Hagerman RJ, Taylor AK, Gane LW, Godfrey TE, Hagerman PJ. Elevated levels of FMR1 mRNA in carrier males: a new mechanism of involvement in the fragile-X syndrome. Am J Hum Genet. 2000;66:6–15.
31. Kenneson A, Zhang F, Hagedorn CH, Warren ST. Reduced FMRP and increased FMR1 transcription is proportionally associated with CGG repeat number in intermediate-length and premutation carriers. Hum Mol Genet. 2001;10:1449–1454.
32. Concha L, Gross DW, Beaulieu C. Diffusion tensor tractography of the limbic system. AJNR Am J Neuroradiol. 2005;26:2267–2274.
33. Catani M, Jones DK, Daly E, et al. Altered cerebellar feedback projections in Asperger syndrome. Neuroimage. 2008;41:1184–1191.
34. Pugliese L, Catani M, Ameis S, et al. The anatomy of extended limbic pathways in Asperger syndrome: a preliminary diffusion tensor imaging tractography study. Neuroimage. 2009;47:427–434.
35. Aravamuthan BR, Muthusamy KA, Stein JF, Aziz TZ, Johansen-Berg H. Topography of cortical and subcortical connections of the human pedunculopontine and subthalamic nuclei. Neuroimage. 2007;37:694–705.
36. Jissendi P, Baudry S, Baleriaux D. Diffusion tensor imaging (DTI) and tractography of the cerebellar projections to prefrontal and posterior parietal cortices: A study at 3T. J Neuroradiol. 2008;35:9.
37. Taoka T, Kin T, Nakagawa H, et al. Diffusivity and diffusion anisotropy of cerebellar peduncles in cases of spinocerebellar degenerative disease. Neuroimage. 2007;37:387–393.